Colloid Polym Sci (2015) 293:3013–3024
DOI 10.1007/s00396-015-3711-8

ORIGINAL CONTRIBUTION

Preparation of multicompartment micelles from amphiphilic linear triblock terpolymers by pH-responsive self-assembly

Wei Zhang[1] · **Haifeng Bao**[1] · **Jinxin He**[1,2] · **Xia Dong**[1,2]

Received: 21 May 2015 / Revised: 9 July 2015 / Accepted: 11 July 2015 / Published online: 30 July 2015

Abstract Multicompartment micelles, as an intriguing class of self-assembled aggregates with subdivided solvophobic cores, show high potentials for various applications. Their unique morphologies and sequestration properties depend highly on structure and chemical composition of the building blocks as well as self-assembly environments. To further understand their relationships, a series of well-defined amphiphilic triblock terpolymers poly(methyl methacrylate)-*block*-poly(2-(cinnamoyloxy)ethyl methacrylate)-*block*-poly(2-dimethylaminoethyl methacrylate) (PMMA-*b*-PCEMA-*b*-PDMAEMA) was synthesized via sequential atom transfer radical polymerization (ATRP) followed by selective modification of the middle block, and the self-assembly of PMMA-*b*-PCEMA-*b*-PDMAEMA via direct dispersing in water and step-wise procedures through solvent exchange was studied, respectively. Dynamic laser scattering (DLS) studies showed the existence of large-sized aggregates formed through direct self-assembly of PMMA-*b*-PCEMA-*b*-PDMAEMA triblock terpolymers in water, and the aqueous solutions were found to exhibit the surface tension reduction. This is probably caused by the frozen micelles adsorbed on the air/water interface which play the role of Pickering emulsifiers. However, PMMA-*b*-PCEMA-*b*-PDMAEMA multicompartment micelles could be successfully prepared by the step-wise self-assembly method, inhibiting the formation of frozen micelles and large aggregates. Prepared from different PMMA-*b*-PCEMA-*b*-PDMAEMA triblock terpolymers, the homogeneously nano-sized multicompartment micelles of oval morphologies with distinct subdivided core domains were confirmed by transmission electron microscope (TEM). Besides, various morphologies of the multicompartment micelles were obtained simply by altering the pH value of water. This multicompartment micelle system with adjustable pH response holds potential for therapeutic delivery of multiple incompatible drug payloads and is believed to contribute to enriching the research field of tunable polymer self-assemblies.

Keywords ATRP · Self-assembly · Frozen micelle · Multicompartment micelle · pH-responsive

✉ Xia Dong
dongxia@dhu.edu.cn

Wei Zhang
zwphone@sina.com

[1] College of Chemistry, Chemical Engineering and Biotechnology, Donghua University, Shanghai 201620, China

[2] Key Lab of Textile Science and Technology, Ministry of Education, Shanghai 201620, China

Introduction

Applications within the emerging field of nanotechnology, concerning drug and gene delivery systems, nanoreactors, and so on, have increasing demands for new and complex materials with well-defined three-dimensional structure over the size range of 1–1000 nm [1, 2]. Currently, many more designed nanostructures are effectively produced from the self-assembly of block copolymers on interfaces or in solution because of various types of monomers available, ease of chemical reaction control, and especially defined yet modifiable architectures of the macromolecules. Depending on different chemical compositions and blocking sequences of AB coblock copolymers or ABC triblock terpolymers as the building blocks, typical examples of the formed micellar morphologies include core-shell-corona structures, nanotubes, helices, micelles with segregated coronas, and multicompartment micelles [3–8].

The concept of multicompartment micelles draws inspiration from biological systems in which a single eukaryotic cell, comprising several different subunits, can naturally perform an array of distinct functions. Attractively, there are multiple domains in multicompartment micelles with distinct chemical environments existing in close proximity within one nanostructure. They are shown to possess the ability to selectively store and transport small organic molecules within their solvophobic/hydrophobic interior [9, 10]. As an intriguing category of nanoscopically self-assembled aggregates with subdivided solvophobic cores, multicompartment micelles have been studied more and more extensively for their unique morphological properties. Since the key feature of multicompartment micelles is the microphase separation within the hydrophobic core region of the micelles, the most important step to prepare multicompartment micelles from ABC triblock terpolymers is selecting hydrophobic A and B components that are sufficiently incompatible, and thus, will segregate into distinct domains [11]. Laschewsky and co-workers have reported the aqueous self-assembly of an triphilic ABC linear triblock terpolymer poly(4-methyl-4-(4-vinylbenzyl)morpholinium chloride)-block-polystyrene-block-poly(pentafluorophenyl 4-vinylbenzyl ether) (PVBM-*b*-PS-*b*-PVBFP) consisting of strongly incompatible hydrocarbon and fluorocarbon blocks which favor the segregation into distinct domains. This led to "raspberry-like" morphologies consisting of small fluorinated PVBFP nodules (D≈ 3 nm) within a larger PS core (D≈15 nm) [12]. Further studies systematically illustrate all possible morphological variations of the multicompartment micelles provided by varying the blocking sequence of the triphilic terpolymers and the relative length of the blocks [13] as well as the selective solvents (water, isopropanol, acetone, *n*-hexane, etc.) for individual blocks, which afford spherical micelles with "sickle" fluorocarbon domains at the external interface of the core, "soccer ball" morphologies, micelles with "capsule" fluorocarbon domains inside the core, and so forth [14]. Nevertheless, ABC miktoarm star terpolymers provide a versatile and powerful route toward multicompartment micelles, which results from the fact that the miktoarm star architecture effectively suppresses the formation of concentric domains with an "onion-like" arrangement, the default core-shell-corona structure adopted by common ABC linear triblock terpolymers [15, 16]. However, these types of multicompartment micelles mentioned above are mainly prepared from either fluoride-containing triphilic ABC linear triblock terpolymers, or expensive and complex ABC miktoarm star terpolymers. Multicompartment micelles prepared from simple linear ABC triblock terpolymers were seldom reported until Müller and co-workers developed facile strategies toward homogeneous populations of well-defined multicompartment micelles using several kinds of simple commercially available polymers. For each of the triblock terpolymers used to form nanoscale multicompartment micelles, the importance of incompatibility between individual blocks should be highly considered and the selective solvent systems need to be carefully chosen and prepared [17].

The aim of this work is to prepare the multicompartment micelles bearing discrete hydrophobic core domains with a variety of different yet tunable morphologies, from a simple type of amphiphilic ABC linear triblock terpolymer which is entirely synthesized in our laboratory. Herein, we report the formation of core-compartmentalized micelles by the step-wise self-assembly of a designed ABC triblock terpolymer poly(methyl methacrylate)-block-poly(2-(cinnamoyloxy)ethyl methacrylate)-block-poly(2-dimethylaminoethyl methacrylate) (PMMA-*b*-PCEMA-*b*-PDMAEMA), in selective solvents. Each of the self-assembly steps was studied and confirmed via dynamic laser scattering (DLS) and transmission electron microscope (TEM). In addition to Müller's work [17], we have investigated the morphological variations of PMMA-*b*-PCEMA-*b*-PDMAEMA multicompartment micelles with different molecular weights under varied pH conditions, which is believed to contribute to enriching the research field of tunable polymer self-assemblies.

Experimental methods

Materials

Ethyl 2-bromoisobutyrate (EBriB, 98 %, Sinopharm Chemical Reagent co., ltd), N,N,N′,N′,N″-pentamethyldiethylenetriamine (PMDETA, 97 %, Sinopharm Chemical Reagent co., ltd), and Cuprous bromide (CuBr, 97 %, Sinopharm Chemical Reagent co., ltd) were used as purchased. Methyl methacrylate (MMA, 99 %, Sinopharm Chemical Reagent co., ltd), 2-(Trimethylsilyloxy)ethyl methacrylate (HEMA-TMS, 99 %, Aldrich), and dimethylaminoethylmethacrylate (DMAEMA, 99 %, Aldrich) were distilled under reduced pressure prior to polymerization. Anisole, isopropanol, acetone, and all other solvents were purchased from Shanghai Chemical Reagent Company and used as received. All reagents used were commercially available and at analytical grade.

Synthesis of PMMA-Br

In the typical experiment, 10.5 mL (0.099 mol) MMA monomer was placed into a round-bottomed flask equipped with a magnetic stirrer, and 0.09468 g (0.66 mmol) CuBr, 413.8 μL (1.98 mmol) PMDETA, and 95.7 μL (0.66 mmol) EBriB were added in sequence. After being subjected to three freeze-pump-thaw cycles to replace any dissolved oxygen with nitrogen, the flask was sealed and immersed in a thermostatic oil bath at 80 °C. The mixture tuned dark green immediately and became viscous progressively as the reaction went on. After a prescribed time of the polymerization reaction, the mixture was exposed to

air under stirring and diluted with acetone and passed through a column of neutral alumina to remove copper catalyst then precipitated in excess methanol. The collected sample was then dried under vacuum overnight at 50 °C to obtain the purified macro-initiator PMMA-Br (Mn=15,600 g/mol, Mw/Mn=1.33).

Synthesis of PMMA-*b*-PHEMATMS-Br

In the typical experiment, 1.5 g (0.1 mmol) of the PMMA-Br initiator was dissolved with 3 mL anisole in a round-bottomed flask, 0.0143 g (0.1 mmol) CuBr, 80.3 μL (0.3 mmol) PMDETA, and 2 mL HEMA-TMS monomer were added in sequence. After being subjected to three freeze-pump-thaw cycles to replace any dissolved oxygen with nitrogen, the flask was sealed and immersed in a thermostatic oil bath at 120 °C. After 24 h, the polymerization was stopped by exposure to the air and the solution was diluted with acetone. After being passed through the column of neutral alumina, the sample was precipitated in excess petrol ether and dried under vacuum overnight at 50 °C to obtain the diblock copolymer PMMA-PHEMATMS with a bromine end (Mn=31,200 g/mol, Mw/Mn=1.20).

Synthesis of PMMA-*b*-PHEMATMS-*b*-PDMAEMA

PMMA-*b*-PHEMATMS-*b*-PDMAEMA triblock terpolymers were synthesized from further chain extension from PMMA-*b*-PHEMATMS diblock copolymers with an -Br end as the macro-initiator. In the typical experiment, a typical 0.1 mmol of the PMMA-PEMATMS-Br initiator was dissolved with 4 mL anisole, addition of 0.1 mmol CuBr, 0.3 mmol PMDETA, and 4 mL DMAEMA monomer were carried out in sequence. After three freeze-pump-thaw cycles and being sealed, the reaction started at 120 °C. After 5 h, the reaction was stopped by exposure to the air. The solution was diluted with acetone and passed through a column of neutral alumina to remove copper catalyst then precipitated in excess petrol ether. The obtained solid PMMA-*b*-PHEMATMS-*b*-PDMAEMA was dried under vacuum overnight at 50 °C (Mn=58,900 g/mol, Mw/Mn=1.19).

The series of PMMA-*b*-PHEMATMS-*b*-PDMAEMA triblock terpolymers with varied molecular weights was obtained by tuning the molar ratio of monomer/initiator as well as the atom transfer radical polymerization (ATRP) reaction time.

Synthesis of PMMA-*b*-PCEMA-*b*-PDMAEMA

Conversion of PMMA-*b*-PHEMATMS-*b*-PDMAEMA to PMMA-*b*-PCEMA-*b*-PDMAEMA was conducted by selective acidic hydrolysis of the TMS-groups on PCEMA blocks, followed by esterification with cinnamoyl chloride. For sufficient conversion, PMMA-*b*-PHEMATMS-*b*-PDMAEMA (0.5 g) was dissolved in a mixture of 10 mL THF and 10 mL methanol containing 1 mL acetic acid as catalyst. The mixture was stirred for 5 h at room temperature, and quantitative removal of the TMS protective group was confirmed by ^{1}H-NMR analysis. The solvents were removed by evaporation and the newly formed hydroxyl groups of the PHEMA block were reacted with a three-fold excess of cinnamoyl chloride in THF and TEA at room temperature overnight. The resultant PMMA-*b*-PCEMA-*b*-PDMAEMA was purified by dialysis against ethanol overnight then dialyzed against water and freeze-dried.

Preparation of PMMA-*b*-PCEMA-*b*-PDMAEMA aqueous solutions

The synthesized PMMA-*b*-PCEMA-*b*-PDMAEMA triblock terpolymers were directly dissolved in ultrapure water with varied concentration from 1 g/L to 1×10^{-5} g/L, followed by ultrasound treatment for 1 h to ensure a homogeneous distribution of PMMA-*b*-PCEMA-*b*-PDMAEMA in water.

Formation of core-corona micelles

The PMMA-*b*-PCEMA-*b*-PDMAEMA terpolymers were dissolved in isopropanol/acetonitrile (3:1 v/v) and prepared at the concentration of 1 g/L. The as-prepared micellar solutions were annealed at 50 °C for 48 h to ensure an equilibrated system.

Formation of multicompartment micelles

To obtain the self-assembled multicompartment micelles, 5 mL of the as-prepared micellar solution were dialyzed into 2 L ultrapure water at pH 6.86, which is the selective solvent for the PDMAEMA block. To further investigate the pH-responsive self-assembly behavior of the terpolymers, pH of ultrapure water was adjusted to 4 and 9.18, respectively.

Characterization

All ^{1}H Nuclear Magnetic Resonance (^{1}H NMR) spectra were recorded at 300 MHz by Bruker 400-MHz spectrometer at 20 °C using $CDCl_3$ as solvent to confirm the structure and composition of the polymers.

Molecular weight and molecular weight distribution of each sample were obtained via gel permeation chromatography (GPC) on Waters BI-MwA using tetrahydrofuran (HPLC grade) as eluent at 1 mL/min flow rate, and the samples were prepared at the concentration of 4 mg/mL; polystyrene standards were used.

The effective pK_as of PMMA-*b*-PCEMA-*b*-PDMAEMA triblock terpolymers were determined by hydrogen ion titration method [8, 18]. Polymer solutions were titrated between pH 2 and 12 using a standard NaOH 0.75 M solution under continuous stirring. The pH was measured using an Ohaus

Scheme 1 Synthesis route for PMMA-*b*-PCEMA-*b*-PDMAEMA

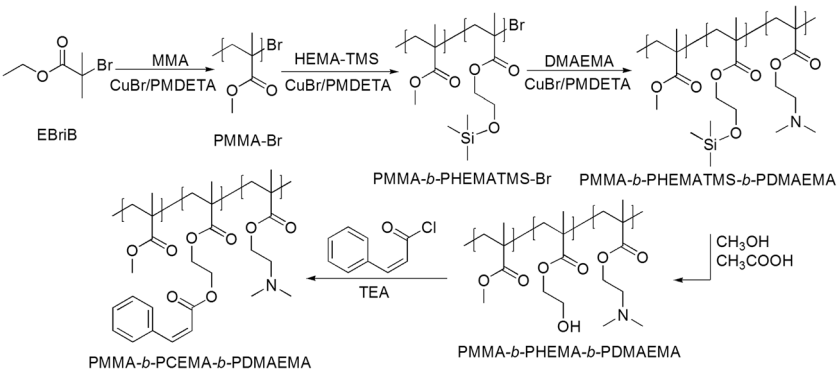

Starter 3C pH meter. The pK_as were calculated as the pH at 50 % ionization.

The equilibrium surface tension of the triblock terpolymer solutions was measured at 25 °C by the Wilhelmy plate technique (Cahn Radian DCA 322 Analyzer, Thermo, USA), and the measurement was carried out until it deviated within ±0.5 mN/m for the last two readings. To ensure equilibrium before the measurements, the solutions were placed in closed environment and stood overnight.

Polymer solubility in different solvents was tested by observation method. At the ambient temperature, 100 mg of the synthesized polymers were placed in the tubes separately and 3 mL of the solvent was then added. The solvents used in the solubility experiment include acetone, ethanol, isopropanol, tetrahydrofuran, acetonitrile, cyclohexane, dichloromethane, and water. Polymers dissolved completely within 3 min were marked as readily soluble (+++), dissolved completely after being heated at 60 °C within 3 min were marked as soluble (++), partially dissolved after being heated at 60 °C were marked as slightly soluble, and those who were unable to be dissolved were marked as insoluble (−).

DLS measurements were performed at a scattering angle of 90° on Brookhaven BI-200SM with a laser operating at a wavelength of λ=532 nm. Before light scattering measurements, all sample solutions were filtered through a polytetrafluoroethylene filter with a pore size of 0.22 μm. All the light scattering experiments were performed at 25 °C.

TEM was performed in bright-field mode on JF2100 electron microscope operated at 200 kV. The samples were prepared by placing one drop of the polymer solution (0.05 g/L) onto carbon-coated copper grid. For selective staining, the TEM specimens were exposed to RuO_4 vapor (stains PCEMA) for 20 min.

Results and discussion

Synthesis of PMMA-*b*-PCEMA-*b*-PDMAEMA triblock terpolymer

Atom transfer radical polymerization is a powerful controlled/living free radical polymerization method used for preparing well-defined polymers with designed structures under moderate

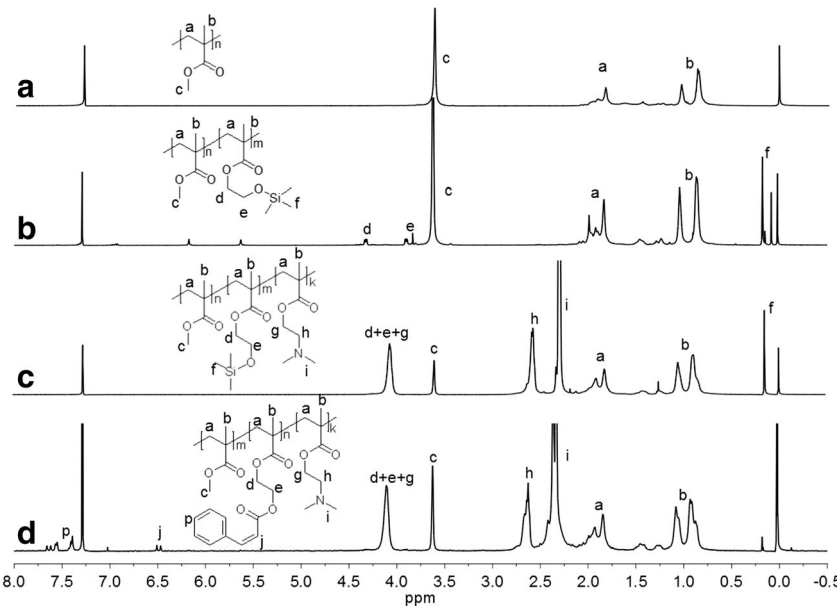

Fig. 1 ^{1}H NMR spectra of **a** PMMA, **b** PMMA-*b*-PHEMATMS, **c** PMMA-*b*-PHEMATMS-*b*-PDMAEMA and **d** PMMA-*b*-PCEMA-*b*-PDMAEMA

conditions [19, 20]. Based on the mechanism of transition metal-mediated equilibrium with halogen atom transferred between the living and the dormant species, polymers with the bromine end were enabled to initiate the ATRP of other serials of monomers leading to block copolymers [21, 22]. The overall synthesis process of poly(methyl methacrylate)-block-poly(2-(cinnamoyloxy)ethyl methacrylate)-block-poly(2-dimethylaminoethyl methacrylate) (PMMA-*b*-PCEMA-*b*-PDMAEMA) by combining successive ATRP of poly(methyl methacrylate)-block-poly(2-(trimethylsilyloxy)ethyl methacrylate)-block-poly(2-dimethylaminoethyl methacrylate) (PMMA-*b*-PHEMATMS-*b*-PDMAEMA) and selective modification of the middle PHEMATMS block is demonstrated in Scheme 1 as a simplified route.

The chemical structures and compositions of PMMA-*b*-PCEMA-*b*-PDMAEMA and its precursors were determined by ^{1}H NMR spectroscopy, as shown in Fig. 1. The chemical shift at 3.63 was ascribed to the –CH_3 connecting the ester groups from PMMA, and the chemical shifts at near 1.9 and 1.0 ppm were ascribed to the –CH_2- and –CH_3 from the main chains of PMMA (Fig. 1a). Figure 1b shows the ^{1}H NMR spectrum of PMMA-*b*-PHEMATMS. Apart from the three typical proton signals of PMMA, the chemical shifts at 4.31, 3.91, and 0.18 ppm were respectively ascribed to the two –CH_2- groups and –CH_3 groups connecting to Si. As shown in Fig. 1c, PMMA-*b*-PHEMATMS-*b*-PDMAEMA gives additional proton signals originating from PDMAEMA compared to PMMA-*b*-PHEMATMS. Typical proton peaks at 4.08 and 2.60 ppm attributed to the –CH_2- groups neighboring to the ester bonds and those neighboring to the –$N(CH_3)_2$ groups peaks at 2.30 ppm attributed to the -CH3 connecting to N from PDMAEMA. Compared to the ^{1}H NMR spectrum of PMMA-*b*-PHEMATMS-*b*-PDMAEMA, ^{1}H NMR spectrum of PMMA-*b*-PCEMA-*b*-PDMAEMA shown in Fig. 1d revealed the new characteristic proton multipeaks at 7.2 to 7.6 ppm, and the peaks at 6.49 ppm attributed to the phenyl groups and double bonds within the cinnamate groups. In addition, the proton signals of -CH_3 within the -$Si(CH_3)_3$ groups diminished, indicating effective conversion of PHEMATMS to PCEMA.

GPC traces as shown in Fig. 2 illustrate that all the molecular weights of the block copolymers were higher than the respective precursors, and no unreacted monomers were detected. Also the traces show that the molecular weights of PMMA-*b*-PCEMA-*b*-PDMAEMAs were slightly higher than the corresponding unfunctionalized PMMA-*b*-PHEMATMS-*b*-PDMAEMAs, suggesting the successful attachment of the cinnamate groups to the middle blocks. The molecular weights and molecular weight distributions (Mw/Mn) of the synthesized PMMA-*b*-PCEMA-*b*-PDMAEMA triblock terpolymers and their precursors are illustrated in Table 1. GPC data show near linear increase of molecular weights with the increasing feed ratio of monomers and reaction time, as well

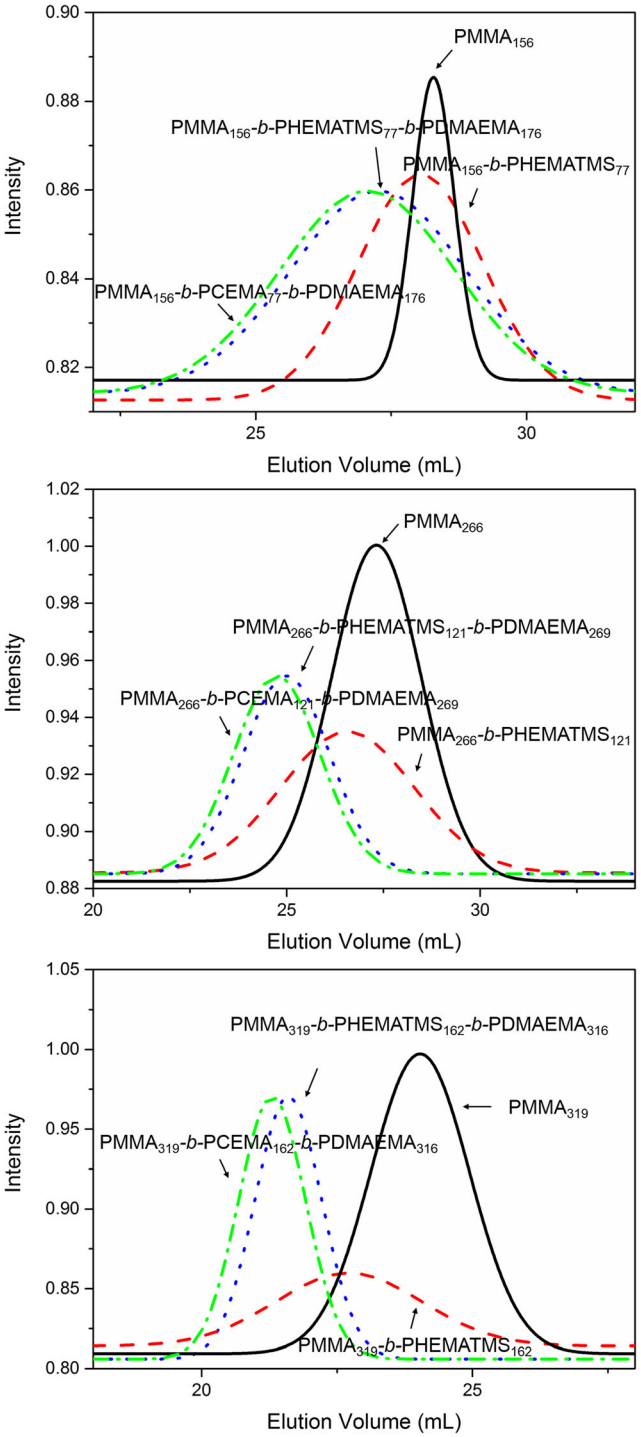

Fig. 2 GPC traces of PMMA-*b*-PCEMA-*b*-PDMAEMAs and their precursors

as relatively narrow molecular weight distributions which is the typical characteristic of ATRP. The molecular weights of PMMA-*b*-PCMEA-*b*-PDMAEMA polymers were larger than those of corresponding unfunctionalized PMMA-*b*-PHEMATMS-*b*-PDMAEMA polymers owing to the large cinnamate groups. All these block polymers afforded narrow polydispersity index. The results indicated that the well-

Table 1 Experimental conditions, Mn, PDI, weight fraction, and effective pK_a of PMMA-*b*-CEMA-*b*-PDMAEMA triblock terpolymers and their precursors

Polymer[a]	Temp. (°C)	Initiator	Molar ratio[b]	Reaction time (h)	Mn (g/mol) [c]	PDI[d]	Weight fraction	Effective pK_a±0.1
M_{156}	80	EBriB	150:1:1:3	1	15,600	1.33	100	–
M_{266}	80	EBriB	250:1:1:3	1	26,600	1.38	100	–
M_{319}	80	EBriB	300:1:1:3	1	31,900	1.37	100	–
$M_{156}H_{77}$	120	M_{156}-Br	300:1:1:3	18	31,200	1.20	50:50	–
$M_{266}H_{121}$	120	M_{266}-Br	300:1:1:3	24	50,700	1.21	53:47	–
$M_{319}H_{162}$	120	M_{319}-Br	300:1:1:3	24	64,600	1.17	49:51	–
$M_{156}H_{77}D_{176}$	120	$M_{156}H_{77}$-Br	500:1:1:3	4	58,900	1.19	27:27:46	–
$M_{266}H_{121}D_{269}$	120	$M_{266}H_{121}$-Br	500:1:1:3	5	92,900	1.21	29:26:45	–
$M_{319}H_{162}D_{316}$	120	$M_{319}H_{162}$-Br	500:1:1:3	5	115,500	1.18	28:28:44	–
$M_{156}C_{77}D_{176}$	–	–	–	–	61,200	1.18	25:30:45	6.9
$M_{266}C_{121}D_{269}$	–	–	–	–	95,500	1.20	28:28:44	6.8
$M_{319}C_{162}D_{316}$	–	–	–	–	120,600	1.18	26:32:42	6.6

[a] M=poly(methyl methacrylate), H=poly(2-(trimethylsilyloxy)ethyl methacrylate), D=poly (2-(dimethylamino)ethyl methacrylate), C=poly(2-cinnamoyloxyethyl acrylate); the numbers in the subscript denote the degrees of polymerization

[b] Molar ratio represents monomer:initiator:CuBr:PMDETA

[c] Mn was determined by GPC measurements with THF as eluent

[d] PDI indicated the polydispersity index of the polymers (Mw/Mn), where weight-average molecular weight (Mw) and number-average molecular weight (Mn) were determined

defined triblock terpolymers bearing photo-crosslinkable cinnamate groups were successfully synthesized. In addition, the effective pK_as of PMMA-*b*-PCEMA-*b*-PDMAEMA triblock terpolymers were between 6.9 and 6.6 (see Table 1), decreasing as the weight fraction of PDMAEMA units decreased. The lower effective pK_as of the polymers was attributed to their greater hydrophobicity because it leads to the reduction of the dielectric constant, rendering ionization more difficult and reducing the pK_a [13, 18].

Self-assembly of PMMA-*b*-PCEMA-*b*-PDMAEMA directly in water

It is well known that typical amphiphilic block copolymers consisting of two different repeating units are usually form core-shell structural micelles, while terpolymers tend to self-assemble into core-shell-corona micelles in water [23, 24]. Hence, the hydrophobic PMMA and PCEMA blocks should form the inner core and shell while the hydrophilic PDMAEMA block forms the corona of the micelles generated in the aqueous solutions. DLS experiments were carried out to confirm the existence and to measure the dynamic radii of the micelles or their aggregates formed by dispersing PMMA-*b*-CEMA-*b*-PDMAEMA triblock terpolymers directly in water. As shown from the experimental results, the hydrodynamic diameters of PMMA-*b*-CEMA-*b*-PDMAEMA triblock terpolymers increase as molecular weight grows at all pH values in the experiment.

At pH 6.86, a near-neutral environment, the average sizes of $PMMA_{156}$-*b*-$PCEMA_{77}$-*b*-$PDMAEMA_{176}$, $PMMA_{266}$-*b*-$PCEMA_{121}$-*b*-$PDMAEMA_{269}$, and $PMMA_{319}$-*b*-$PCEMA_{162}$-*b*-$PDMAEMA_{316}$ were 50, 220, and 373 nm, respectively. Meanwhile, they showed a similar pH-dependent variation, which increases to a larger extent at pH 4 than at pH 9.18 as shown in Fig. 3a–c. In PMMA-*b*-PCEMA-*b*-PDMAEMA terpolymer solutions at pH 4, the image charge effect among the entirely protonated long PDMAEMA chains of the micelles leads to extension and repulsion from each of the corona chains to another, hence, increasing the hydrodynamic radii of the aggregates. However, at pH 9.18, deprotonated PDMAEMA chains become more hydrophobic and have the tendency to shrink. Van der Waals' forces and hydrophobic bonds among the micelles cause firm aggregation of PMMA-*b*-PCEMA-*b*-PDMAEMA triblock terpolymers, while the hydrogen bonds between the coronas and water guarantee that the micelle aggregates are well dispersed in the aqueous solutions [25]. However, the micelles and their aggregates formed by direct dispersing PMMA-*b*-PCEMA-*b*-PDMAEMA triblock terpolymers in water have a large average size and a relatively broad size distribution (notice the diameters in near-neutral water reach micron scale, as shown in Fig. 3b, c).

To examine the amphiphilicity of the synthesized PMMA-*b*-PCEMA-*b*-PDMAEMA triblock terpolymers, surface activity studies were carried out. The equilibrium surface tensions of several PMMA-*b*-PCEMA-*b*-PDMAMEA polymer aqueous solutions versus their

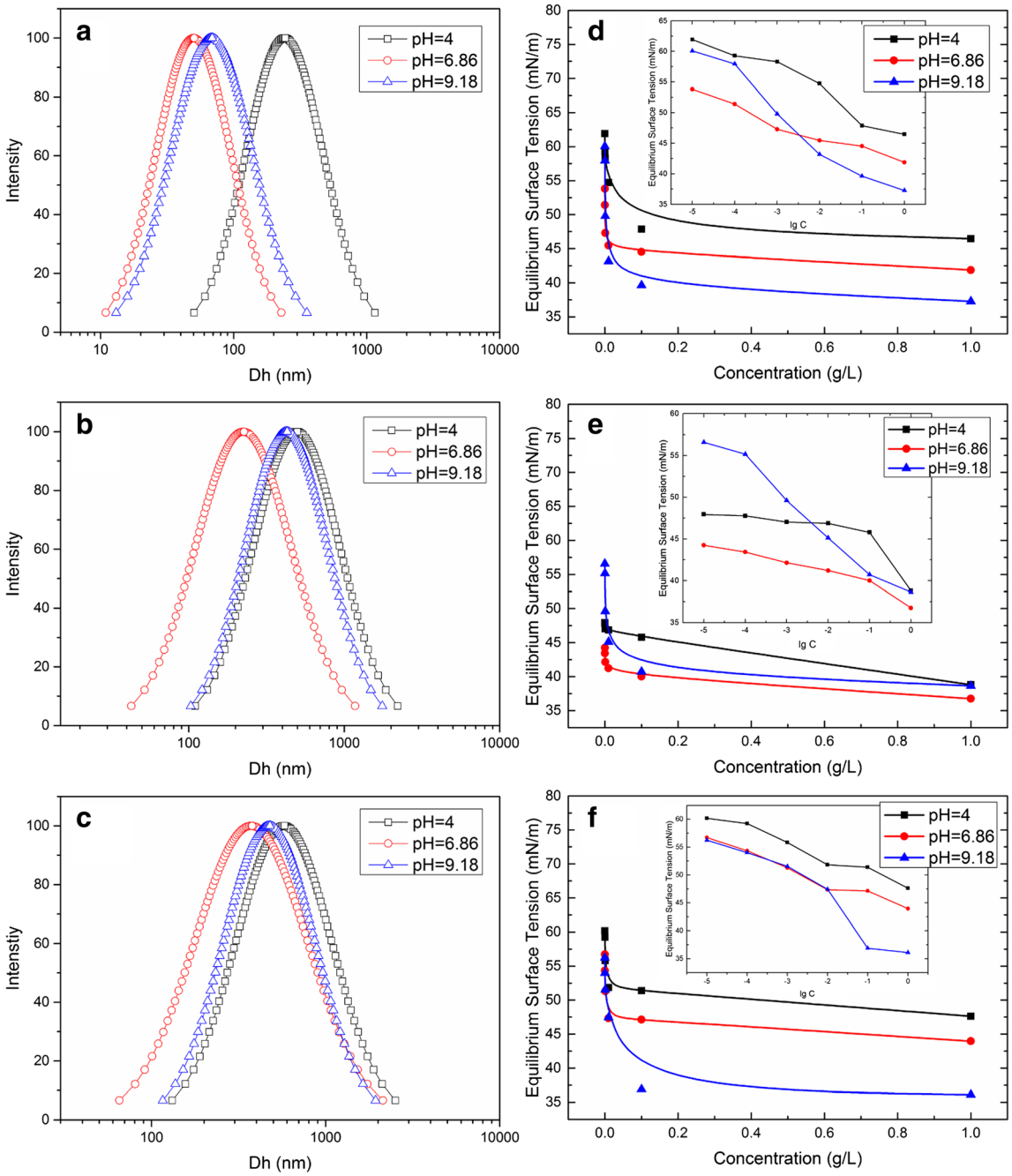

Fig. 3 DLS CONTIN plots of **a** $PMMA_{156}$-*b*-$PCEMA_{77}$-*b*-$PDMAEMA_{176}$, **b** $PMMA_{266}$-*b*-$PCEMA_{121}$-*b*-$PDMAEMA_{269}$ and **c** $PMMA_{319}$-*b*-$PCEMA_{162}$-*b*-$PDMAEMA_{316}$ aqueous solutions at varied pH values; equilibrium surface tension as a function of the concentration of **d** $PMMA_{156}$-*b*-$PCEMA_{77}$-*b*-$PDMAEMA_{176}$, **e** $PMMA_{266}$-*b*-$PCEMA_{121}$-*b*-$PDMAEMA_{269}$ and **f** $PMMA_{319}$-*b*-$PCEMA_{162}$-*b*-$PDMAEMA_{316}$ aqueous solutions at varied pH values

concentrations in ultrapure water at different pH are shown in Fig. 3d–f. In all cases, surface tension declined as polymer concentration increased, until reaching around 35 mN/m. This suggested that the copolymers are surface active and have the characteristics of polymeric surfactants because of slow surface tension decease, limited surface tension reduction power, and non-clear transition points on the surface tension-concentration curves. These resembled our previous investigation on the surface activity of triblock [26]. Some researchers, recently, indicated that the amphiphilic block copolymers with degree of polymerization (DP) larger than 20 showed a non-surface activity while only those with DP less than 20 were surface active; this was mainly due to the formation of dynamically frozen micelles of polymers with a large molecular weight (DP >20), that exhibited the non-surface active nature [27].

However, their experimental results are inconsistent with our observations. In our experiment, the surface activity of the amphiphilic block copolymers was still observed when the degree of polymerization was larger than 20. This inconsistency to our surface activity observation might result from the fact that there remain a few PMMA-*b*-PCEMA-*b*-PDMAEMA frozen micelles adsorbed at the air/water interface, which play the role of Pickering emulsifiers [28, 29]. For the three of the PMMA-*b*-PCEMA-*b*-PDMAEMA triblock terpolymers studied, surface tension reduction power was weakened at pH 4, confirming the existence of the adsorbed PMMA-*b*-PCEMA-*b*-PDMAEMA frozen micelles at the air/water interface. Since the protonated PDMAMEA chains were electrostatically repelled by image charge from the water surface, the adsorbed state at the air/water interface was destabilized, causing a tendency of the frozen micelles to extend in bulk that favor non-surface active nature. This is also proven by the larger average size of the polymers at pH 4 according to DLS plots (Fig. 3 a–c). However, at pH 9.18, the low ionization degree of PDMAEMA chains enabled the firmly frozen micelle layer on the air/solution interface, thus, showing better surface active property [30]. Moreover, when pH level of the aqueous solutions was controlled to the near-pK_a value (pH=6.86), $PMMA_{156}$-*b*-$PCEMA_{77}$-*b*-$PDMAEMA_{176}$ and $PMMA_{319}$-*b*-$PCEMA_{162}$-*b*-$PDMAEMA_{316}$ exhibited similarly gentle trends from the initial surface tension to the low plateau, while $PMMA_{266}$-*b*-$_{121}$-*b*-$PDMAEMA_{269}$ decreased a much larger extent of the surface tension over the concentration range in this experiment. It might be due to the smaller content of hydrophobic chains in $PMMA_{156}$-*b*-$PCEMA_{77}$-*b*-$PDMAEMA_{176}$, as it afforded Pickering particle (frozen micelle) layer that was less stably adsorbed on the air/water interface than $PMMA_{266}$-*b*-$PCEMA_{121}$-*b*-$PDMAEMA_{269}$ did [31]. Meanwhile, $PMMA_{319}$-*b*-$PCEMA_{162}$-*b*-$PDMAEMA_{316}$ exhibited lower surface activity than $PMMA_{266}$-*b*-$PCEMA_{121}$-*b*-$PDMAEMA_{269}$ over the experimental pH range because of its larger molecular weight and more tendency to form frozen micelle aggregates in bulk [32]. Scheme 2 illustrates the direct self-assembly of PMMA-*b*-PCEMA-*b*-PDMAEMA triblock terpolymers in water.

Self-assembly of PMMA-*b*-PCEMA-*b*-PDMAEMA by step-wise method

The formation of frozen micelles and their aggregates through direct self-assembly of PMMA-*b*-PCEMA-*b*-PDMAEMA triblock terpolymers in water might be avoided by a step-wise method of self-assembly that enables the formation of dynamic micelles with microphase segregation. Hence, the solubility test of each of the three blocks of PMMA-*b*-PCEMA-*b*-PDMAEMA triblock terpolymers was carried out to select the suitable solvents precisely. The solubility test results for the three blocks of PMMA-*b*-PCEMA-*b*-PDMAEMA triblock terpolymers are summarized in Table 2. Isopropanol/acetonitrile is a non-solvent for the middle PCEMA block, and water is a non-solvent for both blocks PMMA and PCEMA. To obtain well-defined multicompartment micelles, the procedures included annealing treatment in isopropanol/acetonitrile and subsequent dialysis into water. It enables gradual exposure, rather than direct dissolution, to the non-solvent (water) for the hydrophobic PCEMA and PMMA blocks. The procedures avoided undesirable kinetic traps by step-wise reduction of the degrees of freedom for the micelle formation of PMMA-*b*-PCEMA-*b*-PDMAEMA triblock terpolymers [17, 33], and varied morphologies of the multicompartment micelles were observed in this experiment.

The hydrodynamic diameter variation of PMMA-*b*-PCEMA-*b*-PDMAEMA self-assemblies was investigated by DLS measurement. After the 48-h annealing treatment in the mixture of isopropanol and acetonitrile (3:1 v/v), the average sizes of $PMMA_{156}$-*b*-$PCEMA_{77}$-*b*-$PDMAEMA_{176}$, $PMMA_{266}$-*b*-$PCEMA_{121}$-*b*-$PDMAEMA_{269}$, and $PMMA_{319}$-*b*-$PCEMA_{162}$-*b*-$PDMAEMA_{316}$ micelles were 9.3, 10.7, and 12.8 nm, respectively, which increased with the growth of molecular weight, while kept generally homogeneous in the small nanometer range, as shown in Fig. 4a. The molecular-weight-dependent increase trend was also observed from the size variation of the micelles formed after being dialyzed into water. Besides, three of $PMMA_{156}$-*b*-$PCEMA_{77}$-*b*-$PDMAEMA_{176}$, $PMMA_{266}$-*b*-$PCEMA_{121}$-*b*-$PDMAEMA_{269}$, and $PMMA_{319}$-*b*-$PCEMA_{162}$-*b*-$PDMAEMA_{316}$ micelles all became larger with relatively narrow diameter distribution

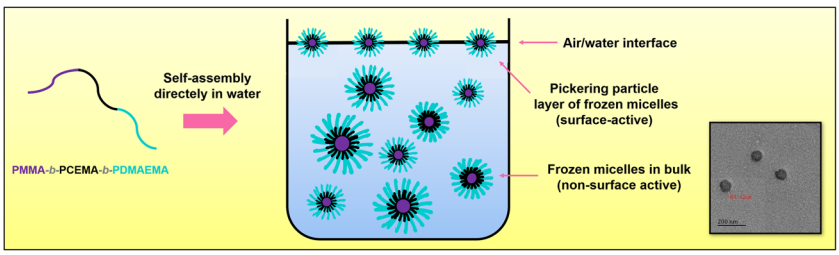

Scheme 2 Schematic illustration of self-assembly of PMMA-*b*-PCEMA-*b*-PDMAEMA triblock terpolymers directly in water; the inset is a TEM image of core-shell-corona micelles self-assembled from $PMMA_{266}$-*b*-$PCEMA_{121}$-*b*-$PDMAEMA_{269}$ directly in water

Table 2 Polymer solubility test results

Solvent	PMMA	PCEMA	PDMAEMA
Isopropanol	+	–	+++
Acetonitrile	+++	+	+++
Isopropanol/Acetonitrile (3:1 v/v)	++	–	+++
Water	–	–	+++

+++ Readily soluble, ++ soluble, + partially soluble, − insoluble

after the dialysis treatment, as shown in Fig. 4b. For instance, the hydrodynamic diameter of $PMMA_{156}$-*b*-$PCEMA_{77}$-*b*-$PDMAEMA_{176}$ multicompartment micelles reached 31.8 nm after being dialyzed into water, showed a nearly three-fold increase approximately, which implied the morphological transition or regular stacking of the micelles took place during the solvent exchange. For $PMMA_{266}$-*b*-$PCEMA_{121}$-*b*-$PDMAEMA_{269}$ and $PMMA_{319}$-*b*-$PCEMA_{162}$-*b*-$PDMAEMA_{316}$, the average sizes came up to 32.1 and 38.8 nm, respectively.

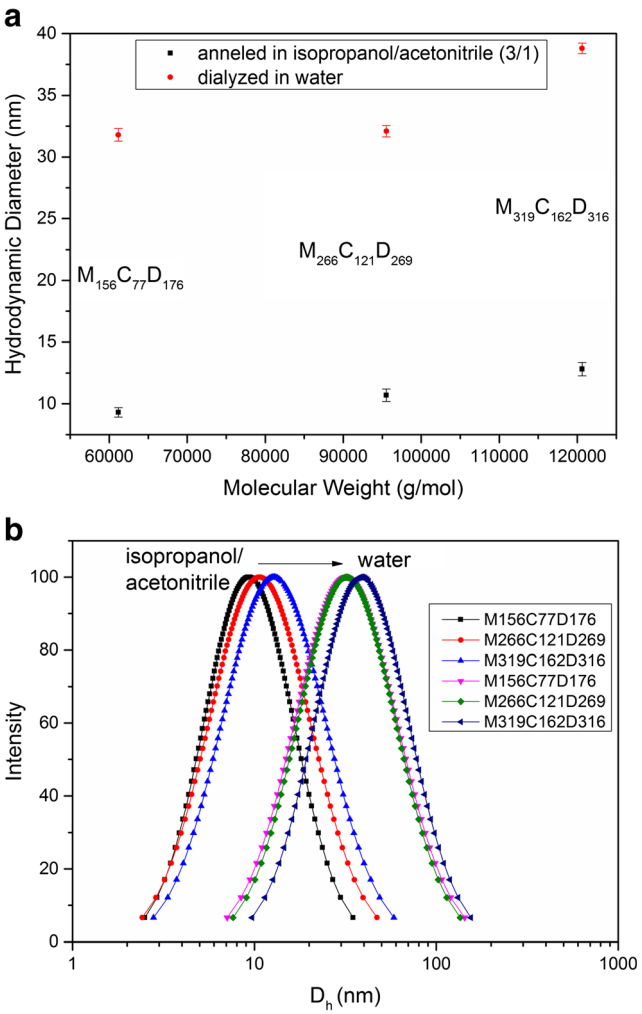

Fig. 4 **a** The variation of hydrodynamic diameters of PMMA-*b*-PCEMA-*b*-PDMAEMA annealed in isopropanol/acetonitrile and further dialyzed in water. **b** DLS CONTIN plots of PMMA-*b*-PCEMA-*b*-PDMAEMA annealed in isopropanol/acetonitrile and further dialyzed in water

In addition to the size increase following the solvent exchange from isopropanol/acetonitrile to water, morphology variations of the mainly investigated $PMMA_{266}$-*b*-$PCEMA_{121}$-*b*-$PDMAEMA_{269}$ triblock terpolymer were detected by transmission electron microscopy. Figure 5 displays the TEM micrographs of $PMMA_{266}$-*b*-$PCEMA_{121}$-*b*-$PDMAEMA_{269}$ triblock terpolymer after being annealed in isopropanol/acetonitrile (Fig. 5a) and dialyzed in water (Fig. 5b, c), with RuO_4 staining. RuO_4 only stains double bonds and aromatic groups within the middle PCEMA block, so the contrast to light gray PMMA and invisible PDMAEMA is enhanced that helps identify the microphase segregated blocks.

$PMMA_{266}$-*b*-$PCEMA_{121}$-*b*-$PDMAEMA_{269}$ triblock terpolymer dissolved in a non-solvent for the PCEMA middle block (acetonitrile/isopropanol) yielded core-corona structural micelles with a PCEMA core and a mixed PMMA/PDMAEMA corona. As Fig. 5a shows, the black dots are the stained PCEMA cores with a diameter of approximately 8 to 10 nm, surrounded by a mixed PMMA/PDMAEMA coronas which are hard to identify due to beam degradation. During subsequent dialysis of these core-corona micelles into a non-solvent for both PMMA and PCEMA, self-assembly took place: the PMMA/PDMAEMA patches of the corona rearranged to minimize the energetically unfavorable PMMA/non-solvent interface, inducing aggregation along the exposed PMMA patches, which stimulated clustering into homogeneously oval multicompartment micelles with microphase separation (Fig. 5b). $PMMA_{266}$-*b*-$PCEMA_{121}$-*b*-$PDMAEMA_{269}$ multicompartment micelles have discrete domains of PCEMA compartments (black), as shown more clearly in Fig. 5c. However, as Fig. 5d shows, the cores of $PMMA_{266}$-*b*-$PCEMA_{121}$-*b*-$PDMAEMA_{269}$ multicompartment micelles shrink at pH 4, and the two black regions of PCEMA are closer. Herein, the completed protonated PDMAEMA coronas stabilized $PMMA_{266}$-*b*-$PCEMA_{121}$-*b*-$PDMAEMA_{269}$ multicompartment micelles with electrostatic repulsion (pK_a is 6.8±0.1 as shown in Table 1). Meanwhile inside the micelles, the compartmentalized core was contracted and the PCEMA patches clustered spontaneously to reduce the area of PMMA/water and PCEMA/water interfaces, induced by the decrease in pH.

Apart from the oval multicompartment micelles formed by self-assembly of $PMMA_{266}$-*b*-$PCEMA_{121}$-*b*-$PDMAEMA_{269}$ core-corona micelles, another type of multicompartment micelles had been found through TEM observation. Figure 6a displays the multicompartment micelles of $PMMA_{319}$-*b*-$PCEMA_{162}$-*b*-$PDMAEMA_{316}$ triblock terpolymer. With a slightly larger average size compared to $PMMA_{266}$-*b*-$PCEMA_{121}$-*b*-$PDMAEMA_{269}$ multicompartment micelles (also see Fig. 4b), $PMMA_{319}$-*b*-$PCEMA_{162}$-*b*-$PDMAEMA_{316}$ multicompartment micelles also exhibit a generally oval

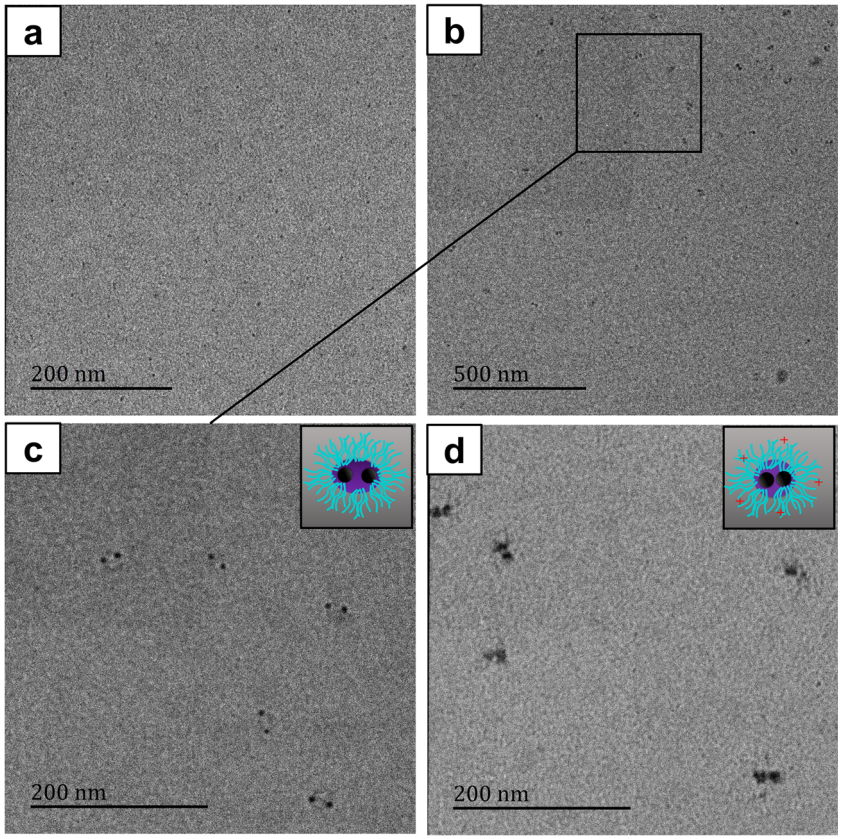

Fig. 5 TEM images of $PMMA_{266}$-*b*-$PCEMA_{121}$-*b*-$PDMAEMA_{269}$ **a** annealed in isopropanol/acetonitrile (3:1 v/v), **b**, **c** dialyzed in water, and **d** dialyzed in water at pH 4 (RuO_4 staining: PCEMA *black*, PMMA *bright gray*, PDMAEMA *light gray*)

structure. PMMA core of the main population (highlighted by the red-dashed circles) is compartmented by a monolithic PCEMA patch as shown more clearly in Fig. 6b.

During the annealing procedure, $PMMA_{319}$-*b*-$PCEMA_{162}$-*b*-$PDMAEMA_{316}$ triblock terpolymers underwent the formation of core-corona micelles, similar to $PMMA_{266}$-*b*-$PCEMA_{121}$-*b*-$PDMAEMA_{269}$ (TEM image omitted). However, subsequent dialysis led to another morphology of self-assembly, different from $PMMA_{266}$-*b*-$PCEMA_{121}$-*b*-$PDMAEMA_{269}$. The difference in morphology between $PMMA_{319}$-*b*-$PCEMA_{162}$-*b*-$PDMAEMA_{316}$ and $PMMA_{266}$-*b*-$PCEMA_{121}$-*b*-$PDMAEMA_{269}$ multicompartment micelles might be attributed to the different proportion of the middle PCEMA block within the two triblock terpolymers that had influenced the self-assembly process during the solvent change: the PCEMA block weight fractions in $PMMA_{319}$-*b*-$PCEMA_{162}$-*b*-$PDMAEMA_{316}$ and $PMMA_{266}$-*b*-$PCEMA_{121}$-*b*-$PDMAEMA_{269}$ are 0.28 and 0.32, respectively. During the dialysis procedure, both of $PMMA_{266}$-*b*-$PCEMA_{121}$-*b*-$PDMAEMA_{269}$ and $PMMA_{319}$-*b*-$PCEMA_{162}$-*b*-$PDMAEMA_{316}$ had gone through the PMMA/PDMAEMA corona rearrangement to minimize the unfavorable PMMA/non-solvent interface. The red-dashed triangular frames in Fig. 6a mark fusion events of the core-corona micelles during the self-assembly. Eventually, core-corona micelles clustered into multicompartment micelles, along with

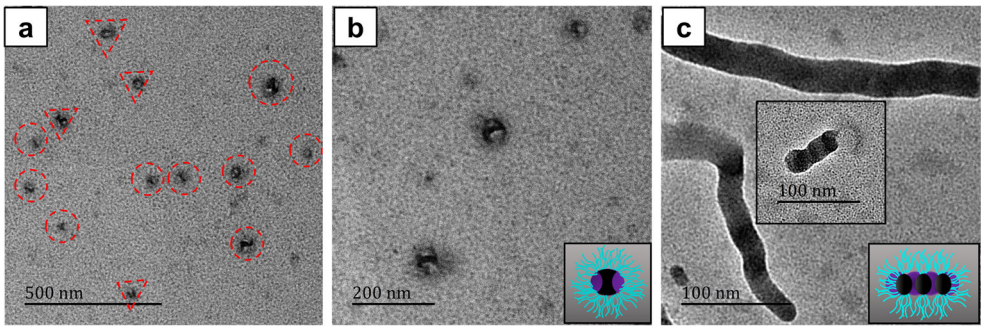

Fig. 6 TEM images of $PMMA_{319}$-*b*-$PCEMA_{162}$-*b*-$PDMAEMA_{316}$ dialyzed (after annealing in isopropanol/acetonitrile) in water **a**, **b** at pH 6.86, and **c** at pH 9.18 (RuO_4 staining: PCEMA *black*, PMMA *bright gray*, PDMAEMA *light gray*)

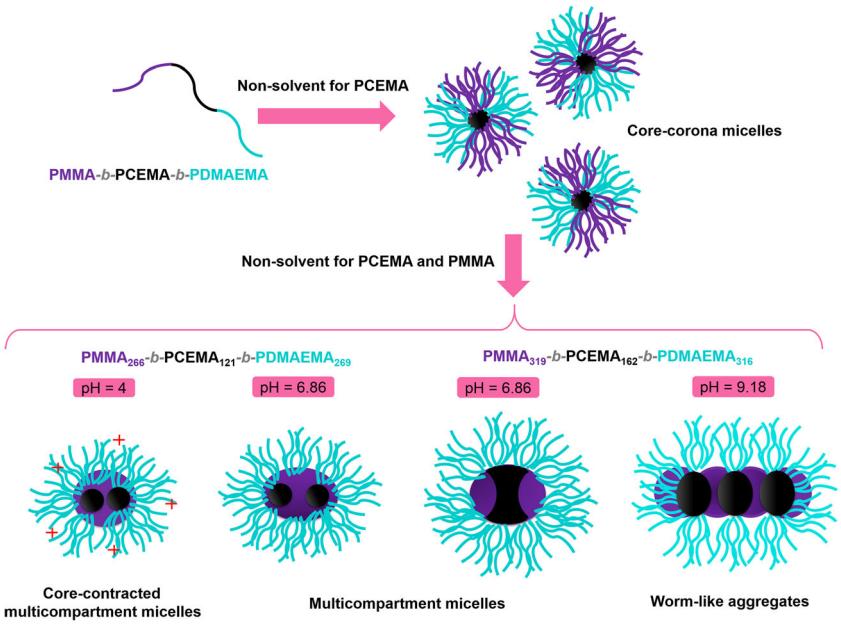

Scheme 3 Schematic illustration of micellization with microphase segregation of PMMA-*b*-PCEMA-*b*-PDMAEMA triblock terpolymers and pH-responsive formation of the multicompartment micelles

PMMA patches aggregating into a core embraced in the PDMAEMA corona. As for self-assembly of $PMMA_{319}$-*b*-$PCEMA_{162}$-*b*-$PDMAEMA_{316}$ core-corona micelles, the hydrophobic PCEMA patches are so large that they gather together to be conjunct as a whole, resulting in compartmenting the PMMA core from the middle of it rather than existing in discrete domains. Although stabilized homogeneously in nanoscale range, $PMMA_{319}$-*b*-$PCEMA_{162}$-*b*-$PDMAEMA_{316}$ multicompartment micelles are sensitive to pH increase. When the pH value was adjusted to 9.18, the PDMAEMA corona was uncharged and contracted that induced the side-by-side assembly of $PMMA_{319}$-*b*-$PCEMA_{162}$-*b*-$PDMAEMA_{316}$ multicompartment micelles into warm-like linear aggregates as shown in Fig. 6c. Scheme 3 illustrates the proposed mechanism of morphology evolution of stepwise self-assembly of PMMA-*b*-PCEMA-*b*-PDMAEMA triblock terpolymers.

Conclusions

A series of tirblock terpolymers PMMA-*b*-PCEMA-*b*-PDMAMEA with designed molecular weight and narrow polydispersity has been synthesized successfully, which is confirmed by HNMR analysis and GPC measurement. Direct dissolution of the polymers into water yields self-assemblies with the average sizes of from 50 to 373 nm as molecular weight increases. Inconsistent to the non-surface active nature of polymers with a DP larger than 20 that form dynamically frozen micelles in water, the series of PMMA-*b*-PCEMA-*b*-PDMAMEA show the surface active property, resulting from the few frozen micelles adsorbed at the air/water interface, which was weakened by the image charge effect between the micelle corona and the water surface at a lower pH value. Annealing in isopropanol/acetonitrile (3:1 v/v) ensured a homogeneous equilibrium of core-corona micelles assembled from PMMA-*b*-PCEMA-*b*-PDMAMEA molecules, with an average diameter below 10 nm; subsequent dialysis into water triggered the formation of multicompartment micelles with an average diameter of 30 to 40 nm, inside which the PCEMA and PMMA blocks formed the compartmented hydrophobic core. The tunable structures of the hydrophobic core within the multicompartment micelles were realized by changing the middle PCEMA block length. Besides, the pH-sensitive PDMAEMA corona induced the reversible morphological transition of the multicompartment micelles, which leaded to core-contracted multicompartment micelles at low pH and worm-like aggregates at high pH, respectively. Based on the features, there is the potential application for the therapeutic delivery of multiple incompatible drug payloads. Also, the ability to achieve separate chemical environments within one nanostructure may also afford unique nanocatalysis opportunities.

Acknowledgments This research was supported by the National Nature Science Foundation of China (20973036, 21303013), the Science and Technology Commission of Shanghai Municipality (13ZR1450900), the Fundamental Research Funds for the Central Universities (2232014D3-12), and the National Undergraduate Training Programs for Innovation and Entrepreneurship (201410255050).

References

1. Ober CK, Cheng SZD, Hammond PT, Muthukumar M, Reichmanis E, Wooley KL, Lodge TP (2009) Research in macromolecular science: challenges and opportunities for the next decade. Macromolecules 42(2):465–471
2. Wyman IW, Liu GJ (2013) Micellar structures of linear triblock terpolymers: three blocks but many possibilities. Polymer 54(8): 1950–1978
3. Moughton AO, Hillmyer MA, Lodge TP (2012) Multicompartment block polymer micelles. Macromolecules 45(1):2–19
4. Wang L, Huang H, He T (2014) ABC triblock terpolymer self-assembled core-shell-corona nanotubes with high aspect ratios. Macromolecular rapid communications 35(16):1387–1396
5. Zhu YT, Yang XP, Kong WX, Sheng YP, Yan N (2012) Segmented and double-helix multicompartment micelles from self-assembly of blends of ABC and AB block copolymers in C block-selective solvents. Soft Matter 8(43):11156–11162
6. Yu B, Deng J, Li B, Shi AC (2014) Patchy nanoparticles self-assembled from linear triblock copolymers under spherical confinement: a simulated annealing study. Soft Matter 10(35):6831–6843
7. Zhao XB, Liu P (2015) Reduction-responsive core-shell-corona micelles based on triblock copolymers: Novel synthetic strategy, characterization, and application as a tumor microenvironment-responsive drug delivery system. Acs Appl mater inter 7(1):166–174
8. Fleischli FD, Ghasdian N, Georgiou TK, Stingelin N (2015) Tailoring the optical properties of poly(3-hexylthiophene) by emulsion processing using polymeric macrosurfactants. J Mater Chem C 3(9):2065–2071
9. Torchilin VP (2004) Targeted polymeric micelles for delivery of poorly soluble drugs. Cellular and molecular life sciences: CMLS 61(19–20):2549–2559
10. Chi Y, Scroggins ST, Frechet JM (2008) One-pot multi-component asymmetric cascade reactions catalyzed by soluble star polymers with highly branched non-interpenetrating catalytic cores. Journal of the American Chemical Society 130(20):6322–6323
11. Laschewsky A (2003) Polymerized micelles with compartments. Curr Opin Colloid In 8(3):274–281
12. Kubowicz S, Baussard JF, Lutz JF, Thunemann AF, von Berlepsch H, Laschewsky A (2005) Multicompartment micelles formed by self-assembly of linear ABC triblock copolymers in aqueous medium. Angewandte Chemie 44(33):5262–5265
13. Ward MA, Georgiou TK (2013) Multicompartment thermoresponsive gels: does the length of the hydrophobic side group matter? Polymer Chemistry 4(6):1893–1902
14. Marsat JN, Heydenreich M, Kleinpeter E, Berlepsch HV, Bottcher C, Laschewsky A (2011) Self-assembly into multicompartment micelles and selective solubilization by hydrophilic-lipophilic-fluorophilic block copolymers. Macromolecules 44(7):2092–2105
15. Hanisch A, Groschel AH, Fortsch M, Drechsler M, Jinnai H, Ruhland TM, Schacher FH, Muller AH (2013) Counterion-mediated hierarchical self-assembly of an ABC miktoarm star terpolymer. ACS nano 7(5):4030–4041
16. Wang L, Xu R, Wang ZL, He XH (2012) Kinetics of multicompartment micelle formation by self-assembly of ABC miktoarm star terpolymer in dilute solution. Soft Matter 8(45): 11462–11470
17. Groschel AH, Schacher FH, Schmalz H, Borisov OV, Zhulina EB, Walther A, Muller AH (2012) Precise hierarchical self-assembly of multicompartment micelles. Nature Communications 3:710
18. Ward MA, Georgiou TK (2010) Thermoresponsive terpolymers based on methacrylate monomers: effect of architecture and composition. J Polymer Science Part A: Polymer Chemistry 48(4):775–783
19. Matyjaszewski K (2009) Controlled radical polymerization: state of the art in 2008. Acs Sym Ser 1023:3–13
20. Matyjaszewski K (2012) Atom transfer radical polymerization (ATRP): current status and future perspectives. Macromolecules 45(10):4015–4039
21. Davis KA, Matyjaszewski K (2001) ABC triblock copolymers prepared using atom transfer radical polymerization techniques. Macromolecules 34(7):2101–2107
22. Yang P, Armes SP (2014) Preparation of well-defined poly(2-hydroxyethyl methacrylate) macromonomers via atom transfer radical polymerization. Macromolecular rapid communications 35(2): 242–248
23. Uchman M, Stepanek M, Prochazka K, Mountrichas G, Pispas S, Voets IK, Walther A (2009) Multicompartment nanoparticles formed by a heparin-mimicking bock terpolymer in aqueous solutions. Macromolecules 42(15):5605–5613
24. Xie HQ, Xie D, Chen XY, Guo JS (2005) Synthesis, characterization, and properties of two component amphiphilic polyoxyethylene-containing multiblock copolymers. J Appl Polym Sci 95(6):1295–1301
25. Bagheri M, Pourmoazzen Z, Entezami AA (2013) pH-responsive nanosized-micelles based on poly (monomethylitaconate)-co-poly(dimethylaminoethyl methacrylate) and cholesterol side chains effect on pH change-induced release of piroxicam. J Polym Res 20(9)
26. Dong X, Zhang W, Zong Q, Liu Q, He J (2014) Physicochemical and emulsifying properties of "extended" triblock copolymers. Colloid and Polymer Science 293(2):369–379
27. Matsuoka H, Chen H, Matsumoto K (2012) Molecular weight dependence of non-surface activity for ionic amphiphilic diblock copolymers. Soft Matter 8(35):9140–9146
28. Binks BP, Lumsdon SO (2001) Pickering emulsions stabilized by monodisperse latex particles: effects of particle size. Langmuir: the ACS Journal of surfaces and colloids 17(15):4540–4547
29. Binks BP, Rocher A (2010) Stabilisation of liquid-air surfaces by particles of low surface energy. Phys Chem Chem Phys: PCCP 12(32):9169–9171
30. Tang J, Lee MF, Zhang W, Zhao B, Berry RM, Tam KC (2014) Dual responsive pickering emulsion stabilized by poly[2-(dimethylamino)ethyl methacrylate] grafted cellulose nanocrystals. Biomacromolecules 15(8):3052–3060
31. Ding W, Liu K, Liu XJ, Luan HX, Lv CF, Yu T, Qu GM (2013) Micellization behavior of ionic liquid surfactants with two hydrophobic tail chains in aqueous solution. J Appl Polym Sci 129(4): 2057–2062
32. Halacheva SS, Penfold J, Thomas RK, Webster JR (2012) Effect of polymer molecular weight and solution pH on the surface properties of sodium dodecylsulfate-poly(ethyleneimine) mixtures. Langmuir: the ACS J of surfaces and colloids 28(42):14909–14916
33. Groschel AH, Walther A, Lobling TI, Schmelz J, Hanisch A, Schmalz H, Muller AH (2012) Facile, solution-based synthesis of soft, nanoscale Janus particles with tunable Janus balance. J Am Chem Soc 134(33):13850–13860